JOURNAL OF
Materials
CHEMISTRY

Layered hybrid nickel phyllosilicates and reactivity of the gallery space

Maria G. da Fonseca,†[a] César R. Silva,[b] José S. Barone[b] and Claudio Airoldi*[b]

[a]*Faculdade de Ciências e Tecnologia, Departamento de Química, Universidade Estadual da Paraíba, Campina Grande, Paraíba, Brazil*
[b]*Instituto de Química, Universidade Estadual de Campinas, Caixa Postal 6154, 13083-970 Campinas, São Paulo, Brazil. E-mail: airoldi@iqm.unicamp.br*

Received 28th September 1999, Accepted 14th January 2000

Aminated phyllosilicates have been synthesized by a sol–gel process from reactions of nickel ions and three analogous trialkoxysilanes, 3-(trimethoxysilyl)propylamine, *N*′-[3-(trimethoxysilyl)propyl]ethylenediamine and *N*′-[3-(trimethoxysilyl)propyl]diethylenetriamine, in aqueous basic medium at 298 and 323 K. The inorganic–organic hybrids SILNix ($x = 1$–3) were denoted following the above sequence of aminated silanes, varying from one to three amino groups on the organosilanes. The amount of nickel in the SILNix matrices showed the presence of cations in two different environments: (i) octahedral sites and (ii) in the gallery space complexed by amino groups. The thermal stability decreased in the order SILNi1 > SILNi2 ≈ SILNi3. The basal peaks were associated with lamellar distances of 1.64, 2.15 and 2.45 nm for SILNix ($x = 1$–3), respectively. For the phyllosilicates obtained at room temperature, the values were 1.36 and 1.96 nm for SILNi1* and SILNi2*, respectively. The increased values observed from $n = 1$ to 3 can be attributed to the presence of organic chains in these new structures, which was confirmed by elemental analysis. The samples showed a peak at $2\theta = 60°$ ($d = 0.16$ nm) indexed to the 060 reflection, characteristic of trioctahedral phyllosilicates. XRD results and IR spectroscopy suggested nickel hydroxide was not obtained. Reactions of the hybrids with 2-pyridinecarbaldehyde were carried out to evaluate the reactivity of the amino groups in the gallery space.

Introduction

Silicate minerals or swelling phyllosilicate minerals have been used as inorganic catalysts for a wide range of chemical reactions and processes.[1] These compounds have been applied as heterogeneous catalysts mainly due to their properties, which are clearly manifested through their cation-exchange behaviour, layer dimensions, shape-selectivity, small particle size and unusual intercalation capability.[2–4] However, distinct smectites such as mica and pyrophyllite-talc groups of minerals have little or no ion exchange capacity.[5]

Some phyllosilicate materials can be synthesized under non-hydrothermal conditions by using organotrialkoxysilanes.[6–10] This synthetic route can be employed to produce layered organoclay-like structures with organophilic functionalities disposed in the interlayer cavities. In these processes, synthetic phyllosilicates have been obtained by a simple low-temperature route, in a direct-synthesis procedure, involving reactions of copolymerization of metallic ions with organosubstitued trialkoxysilanes under alkaline conditions.[6–11]

The organo functionalized clays showed lamellar structures quite similar to those of trioctahedral phyllosilicates, which have an inorganic structure similar to talc. Owing to the fact that these inorganic–organic composites contain organic moieties within the layered region, these materials can be used as host matrices, in contrast to talc or mica. In this connection, using this synthetic route, a great variety of phyllosilicates can be obtained with different metallic cations and trialkoxysilanes as precursors.[11] The nature of the new hybrid, which contains an organic moiety with a desired functionality, strongly depends on the organofunctional trialkoxysilanes used.

Some important investigations report methods to synthesize magnesium or nickel phyllosilicate materials. Natural and synthetic nickel phyllosilicates are well known,[12–16] but only two 2 : 1 layered nickel organosilicates have been briefly described with pendant 3-methacryloxypropyl or 3-glycidoxypropyl groups attached to the inorganic matrix.[7,17]

Nickel phyllosilicates can be prepared, in principle, through a copolymerization reaction involving nickel ions and silicic acid. The control of the Ni/Si ratio of the species in solution is an established method to synthesize nickel phyllosilicates.[6] In such a procedure, stoichiometric Ni/Si ratios of 1.33 or 0.66 give distinct formulations of 2 : 1 or 1 : 1 for the expected nickel phyllosilicates. On the other hand, the use of intermediate values between these leads to a mixture of silicates.[7]

The present study is based on the preparation and characterization of three new nickel phyllosilicates. The hybrids were synthesized using aqueous nickel nitrate solutions and three different analogous trialkoxysilanes: 3-(trimethoxysilyl)propylamine, *N*′-[3-(trimethoxysilyl)propyl]ethylenediamine and *N*′-[3-(trimethoxysilyl)propyl]diethylenetriamine, in basic media. The phyllosilicates are denoted SILNix ($x = 1$–3), respectively, according to the number of aminated groups of the organosilane employed. The reactivity of the amino pendant groups attached to these hybrids was explored by reacting the free amino group with 2-pyridinecarbaldehyde.

Experimental

Chemicals

The silylating agents 3-(trimethoxysilyl)propylamine, *N*′-[3-(trimethoxysilyl)propyl]ethylenediamine and *N*′-[3-(trimethoxysilyl)propyl]diethylenetriamine (Aldrich) were reagent grade. The reagent 2-pyridinecarbaldehyde (Aldrich) was distilled under reduced pressure. All other reagents such as

---

†Present address: Instituto de Química, Universidade Estadual de Campinas, Caixa Postal 6154, 13083-970 Campinas, São Paulo, Brazil. E-mail: gardenia@iqm.unicamp.br.

nickel nitrate hexahydrate (Fluka), methanol and sodium hydroxide (Merck) were used without prior purification.

Synthesis of modified phyllosilicates

Nickel phyllosilicates were synthesized by reacting 0.085 mol of nickel nitrate hexahydrate (*i.e.* a 0.052 mol excess) with 0.033 mol of the silylating agent. The salt was dissolved in 300 cm^3 of bidistilled water and the solution was stirred under heating at 323 K. Then, 23.8 cm^3 of a 1.39 mol dm^{-3} solution of the silane in methanol was slowly added dropwise leading to a green suspension. 500.0 cm^3 of aqueous 0.10 mol dm^{-3} sodium hydroxide solution was then slowly added under stirring while the temperature was maintained at 323 K. The suspension was then aged for 5 days at 323 K and the formed gel was centrifuged, extensively washed with water and dried at 323 K for another 5 days. Green, olive and dark cyan solids were formed for nickel phyllosilicates SILNi*x* ($x = 1$–3), respectively. In another preparation route SILNi1 and SILNi2 were obtained without heating during the addition of silane to the nickel(II) solution, the solids were similarly formed, washed and dried as above.

Reaction with 2-pyridinecarbaldehyde

3.00 g samples of the aminated phyllosilicates were suspended in methanol under a dry nitrogen atmosphere and mechanically stirred at 323 K. To the suspension, 5.0 cm^3 of 2-pyridinecarbaldehyde was added dropwise and the reaction was maintained for 24 h. In the course of the reaction, the suspension became light brown after 3 h. The final product was filtered off, washed with ethanol and dried *in vacuo* for 8 h at 323 K. The brown colour of the obtained materials is more pronounced with an increase in the number of nitrogen atoms attached to the organic chain of the synthesized phyllosilicates.

Characterization

X-Ray diffraction patterns were collected on a Shimadzu model XRD 6000 diffractometer using nickel-filtered Cu-Kα radiation. IR spectra were recorded using a Bomem MB-Series FTIR spectrophotometer with KBr pressed samples. Thermal analyses were performed on a DuPont model 1090 B thermogravimetric apparatus coupled with a thermobalance 951, heating to 1273 K at a rate of 0.17 K s^{-1}. The samples varied in weight from 15.0 to 30.0 mg.

Carbon, nitrogen and hydrogen contents were determined using a Perkin-Elmer PE-2400 microelemental analyser. The amounts of nickel in the hybrids were determined by atomic absorption spectrometry. The samples were digested with hydrofluoric acid and before the resulting solution was analyzed.

Electron microscopy and EDS analysis were performed on ground samples, dispersed by sonication in isopropyl alcohol. In order to examine these non-conducting materials, the samples were coated with a conducting layer of gold and carbon by sputter coating (Plasma Science Inc.). The images were obtained by detection of the secondary electrons in the JEOL JSTM-300 microscope. The distribution maps of nickel in the matrix of the hybrid silicates were obtained by using the EDS technique.

Table 1 Percentages of hydrogen, carbon and nitrogen, the observed (obs.) and calculated (calc.) C/N ratio and *n* the number of pendant groups attached to the hybrids

Hybrid	H %	C %	N %	C/N_{obs}	C/N_{calc}	*n*/mmol g^{-1}
SILNi1	3.85	10.01	4.94	2.40	3.00	3.53
SILNi2	4.52	14.02	7.71	2.12	2.50	2.75
SILNi3	5.62	19.79	9.94	2.30	2.33	2.37
SILNi1*	3.65	6.15	3.70	2.00	3.00	2.55
SILNi2*	4.38	9.38	5.41	2.00	2.50	1.93

*Samples synthesized at room temperature.

Results and discussion

Synthetic route

An excess of nickel cations was added to the solution to avoid competition between the processes of formation of Si–O–Ni bonds and the interlamellar nickel–amine complexes. This procedure was adopted owing to the facility of amino groups to form complexes, as was previously observed during the preconcentration of nickel ions in aqueous solution.[18–20] The classical synthetic route for preparation of hybrids by the sol–gel process uses mild reaction conditions at room temperature.[6–11] However, this procedure was unsuccessful for the preparation of the SILNi3 hybrid. A change in the classical procedure was investigated and two different experimental routes were used: the classical route and a second involving a long aging time at 323 K. These changes in conditions improved the degree of crystallinity and also the yield of the inorganic–organic hybrids formed.

Elemental analysis

From the amount of nitrogen determined in all samples, the number of pendant organic groups on the matrices obtained at 323 K were estimated as 3.53, 2.75 and 2.37 mmol g^{-1} for SILNi*x* ($x = 1$–3), respectively. The relationship between the theoretical and the observed C/N values was lower than expected as shown in Table 1, and the samples synthesized at room temperature Table 1 showed a lower number of organic groups. These results are a good indication of influence of the temperature on the matrices formed.

The results for the nickel contents suggested the presence of this cation in two distinct positions: disposed in octahedral sites and in interlayer regions complexed by nitrogen groups. The difference in the total number of nickel atoms and those in octahedral sites (estimated using the relation $Si/N_{oct} = 1.33$ as in the nickel talc structure) corresponds to the amount of complexed nickel. For these calculations, the silicon content was estimated as a function of the number of moles of organic chain present in the structures.

The amount of nickel for the hybrids obtained at 323 K are shown in Table 2. These values illustrate that increasing the organic chain length in the hybrid structure results in a decrease in the total amount of nickel. Specifically for SILNi2 and SILNi3, the chelating effect results in more stable complexes, so that many possible structures can be formed as illustrated in Fig. 1.

Table 2 Number of moles of nickel (N_{Ni}), silicon (N_{Si}), octahedral nickel ($N_{Ni(Oct)}$), interlamellar nickel ($N_{Ni(Inter)}$) and metal/nitrogen ratio (M/N) in SILNi*x* (1–3) hybrids synthesized at 323 K

Hybrid	N_{Ni}/mmol g^{-1}	N_{Si}/mmol g^{-1}	$N_{Ni(Oct)}$/mmol g^{-1}	$N_{Ni(Inter)}$/mmol g^{-1}	M/N
SILNi1	4.72	3.53	2.65	2.07	0.5
SILNi2	4.56	2.75	2.07	2.49	0.5
SILNi3	3.36	2.37	1.78	1.58	0.5

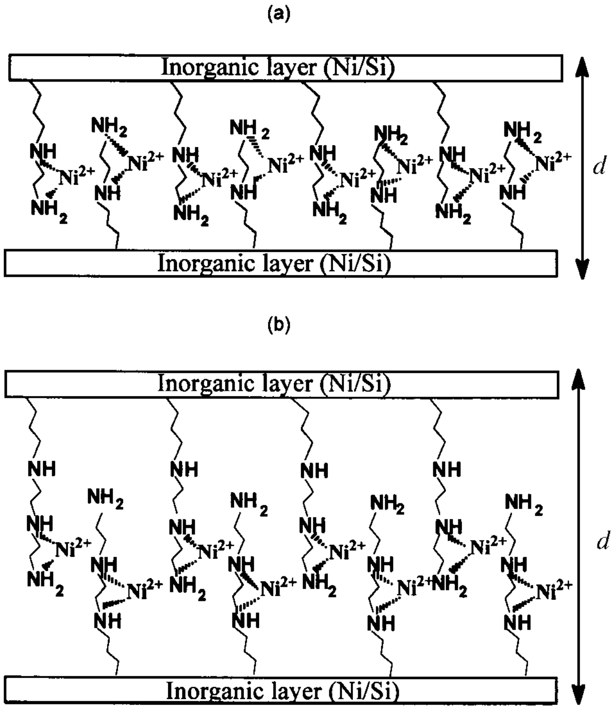

Fig. 1 Proposed types of complexes formed in the interlayer space involving the nitrogen groups (a) in SILNi2 and (b) SILNi3.

XRD diffractometry

The powder diffraction patterns of the synthesized nickel phyllosilicates are illustrated in Fig. 2, where the observed peaks were analysed by comparison with the data obtained for the synthetic nickel talc.[21] The basal peaks were associated with interlayer spacings of 1.64, 2.15 and 2.45 nm for SILNix ($x=1$–3) [Fig. 2(b), (d) and (e), respectively]. For the phyllosilicates obtained at 298 K the values were 1.36 and 1.96 nm for SILNi1* and SILNi2* [Fig. 2(a) and (c), respectively]. Increased values observed for the interlayer spacing in the synthetic hybrids are, therefore, related to the presence of increasingly large organic chains attached to the inorganic backbone.

The synthetic phyllosilicate, nickel talc, has a interlayer spacing of 9.42 nm.[21] We can define a free distance d as the limiting dimension for accommodating an organic guest in the gallery space by $d=d(001)(\text{SILNi}x)-d(001)(\text{nickel talc})$ and values of 0.69, 1.21 and 1.51 nm for SILNi1, SILNi2 and SILNi3 were obtained, respectively. The lengths of the pendant organic groups attached in SILNix were estimated, assuming a zigzag conformation of the organic chain with values of 0.54, 0.94 and 1.20 nm being obtained for $-CH_2CH_2CH_2NH_2$, $-CH_2CH_2CH_2NHCH_2CH_2NH_2$ and $-CH_2CH_2CH_2NHCH_2CH_2NHCH_2CH_2NH_2$, respectively. Assuming that two chains are disposed into the gallery space, a larger interlayer spacing (d) should be observed in all cases; however, the observed free distances indicate that these organic chains are probably organized into interpenetrating bilayers, filling the interlayer space within the Ni/Si inorganic framework.

Increasing the size of the organic chain of a given guest molecule attached to the inorganic matrix led to a corresponding increase in the interlayer spacing. However, the hybrids obtained by the room temperature route showed lower values of interlayer spacing, possibly indicating a decrease in the incorporation of organic groups within the matrix. The phyllosilicate SILNi3 was only formed upon heating to 323 K and the diffractogram [Fig. 2(e)] showed other peaks corresponding to 0.74 and 1.16 nm. Silmilar behaviour was also observed for SILNi2 [Fig. 2(d)], which showed a peak at 0.81 nm. Such features are an indication of layered structures filled with different types of coordination complexes of nickel with the basic centers of the pendant chains. Additionally, the intensity of the lamellar peak, which was higher for samples obtained upon heating, suggested more ordered lamellar structures. The samples showed peaks at $2\theta=60°$ associated with an interplanar distance of 0.16 nm that is characteristic of the 060 reflection. Those data unequivocally indicated the formation of trioctahedral phyllosilicate structures.[22,23]

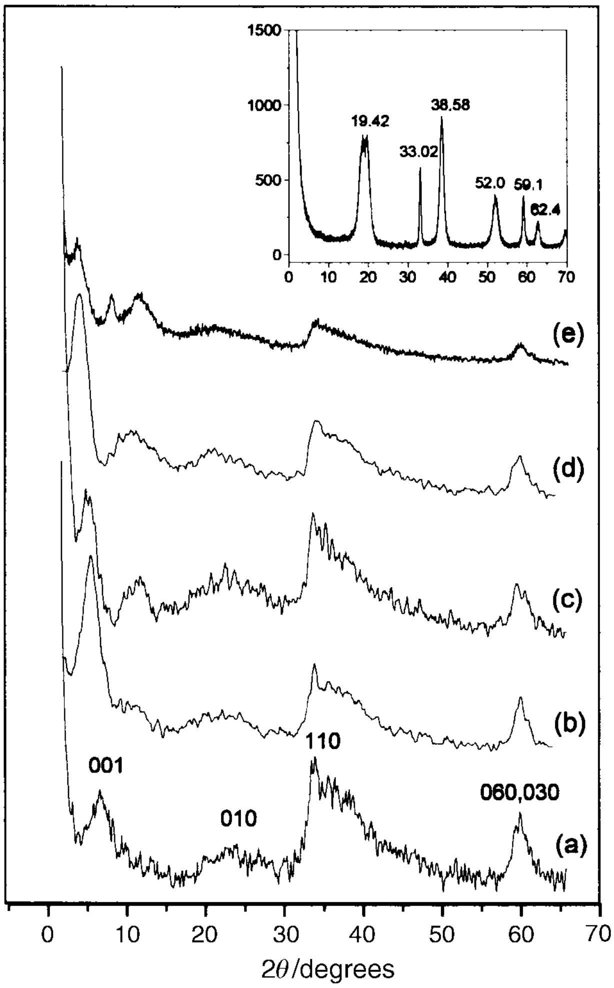

Fig. 2 X-Ray powder diffraction patterns of (a) SILNi1*, (b) SILNi1, (c) SILNi2*, (d) SILNi2 and (e) SILNi3. Hybrids (a) and (c) were synthesized at room temperature. The insert shows the XRD pattern of nickel hydroxide.

After reacting the hybrids SILNix ($x=1$–3) with 2-pyridinecarbaldehyde, the XRD data showed a change in the position of the interlayer spacing peak to 2.55, 2.48 and 3.11 nm, as shown in Fig. 3. This is a good illustration that reaction occurred with the organic moieties located in the interlayer region as shown in Fig. 4. The SILNi2 phyllosilicate was found to show the smallest increase in the lamellar spacing [Fig. 3(b)] and the less effective reaction can be associated with the high number of complexed nickel cations, resulting in a decrease of the number of basic centers available for reaction. This behaviour is expected since cation complexation will lead to a decrease in the electronic density of the nitrogen atoms, making the reaction between 2-pyridinecarbaldehyde and the amino groups more difficult.

Another important observation related to this series of preparations is obtained by considering the possibility of precipitation of nickel hydroxide during the synthetic procedure. This hydroxide is also a layered compound consisting of brucite-like sheets of octahedral nickel with hydroxy groups. β-

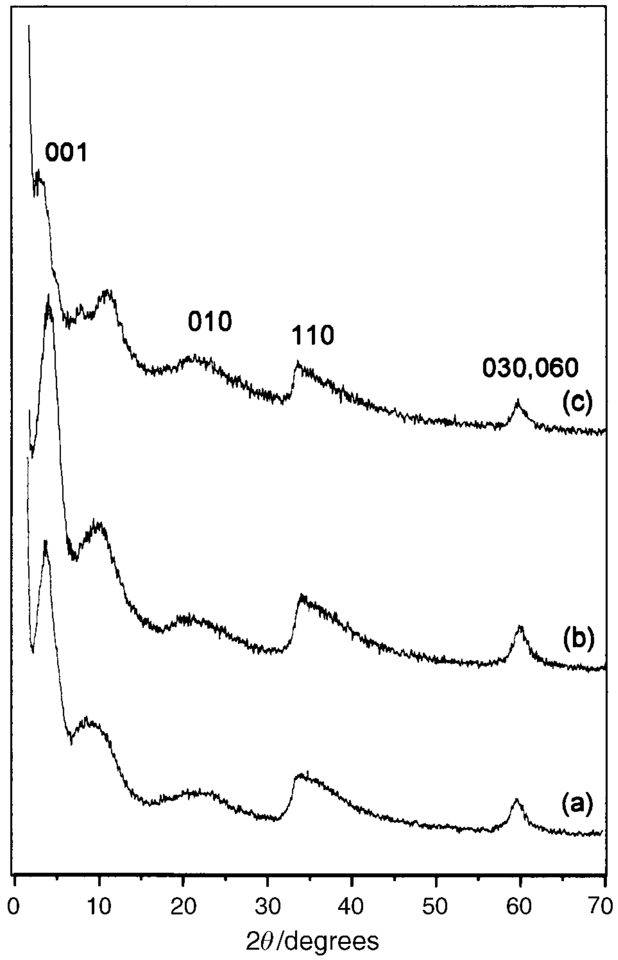

Fig. 3 X-Ray diffraction patterns of phyllosilicates (a) SILNi1, (b) SILNi2 and (c) SILNi3 after reaction with 2-pyridinecarbaldehyde.

and α-Ni(OH)$_2$ forms are possible depending on the layer stacking. β-Ni(OH)$_2$ exhibits a tridimensional structure consisting of stacked brucitic-like layers (00*l* plane) with a *d*(001) basal spacing of 0.46 nm[24] while α-Ni(OH)$_2$, also denoted turbostratic nickel hydroxide, exhibits a bidimensional structure resulting from disordered stacking of the brucitic layers, which are separated by intercalated anionic species.[25,26]

A control experiment was performed by using the same synthetic procedure involving slow addition of sodium hydroxide to the nickel nitrate solution under heating, without alkoxysilane. The precipitate formed was β-Ni(OH)$_2$, identified according to the diffractogram patterns in the insert of Fig. 2. However, for all synthesized phyllosilicates, reflections associated with nickel hydroxide were absent in the diffractograms.[27] These XRD results thus strongly suggest the existence only of modified nickel phyllosilicate.

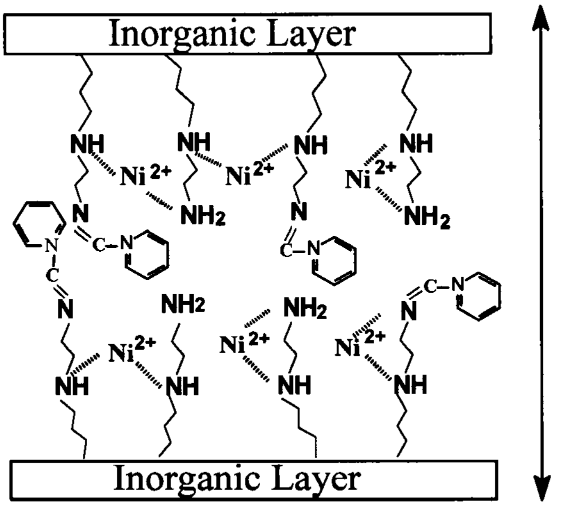

Fig. 4 Representation of the new guest species introduced by reaction with pyridinecarbaldehyde in the gallery space of SILNi2.

Based on XRD results, the suggested structure of the modified nickel phyllosilicates is similar to that of nickel talc [Fig. 5(a)], where tetrahedral–octahedral–tetrahedral arrangements are presented. Nickel cations are located inside octahedral sheets and their coordination is completely *via* oxygen atoms. The organic chains are covalently attached in the modified synthetic phyllosilicate by Si–C bonds, to form tetrahedral CSiO$_3$ groups on the inorganic backbone as shown in Fig. 5(b). These results indicate that the new synthetic hybrids have a layered structure, the interlamellar space of which depends on the type and length of the organic chain molecule R incorporated into the phyllosilicate in these self-organized systems.

IR spectroscopy

IR spectroscopy is a useful technique to detect the integrity of organic moieties of the phyllosilicate within the interlayer and also to confirm the reactions with 2-pyridinecarbaldehyde. The inorganic–organic hybrids showed identical bands as illustrated in Fig. 6. The presence of water intercalated between the layers inhibits the ν(OH) vibration band at 3645 cm^{-1} and a broad band at 3420–3270 cm^{-1} is evident. Only for the SILNi1* phyllosilicate [Fig. 6(a)] was a sharp band observed at 3645 cm^{-1}, which is associated with the hydroxy stretching

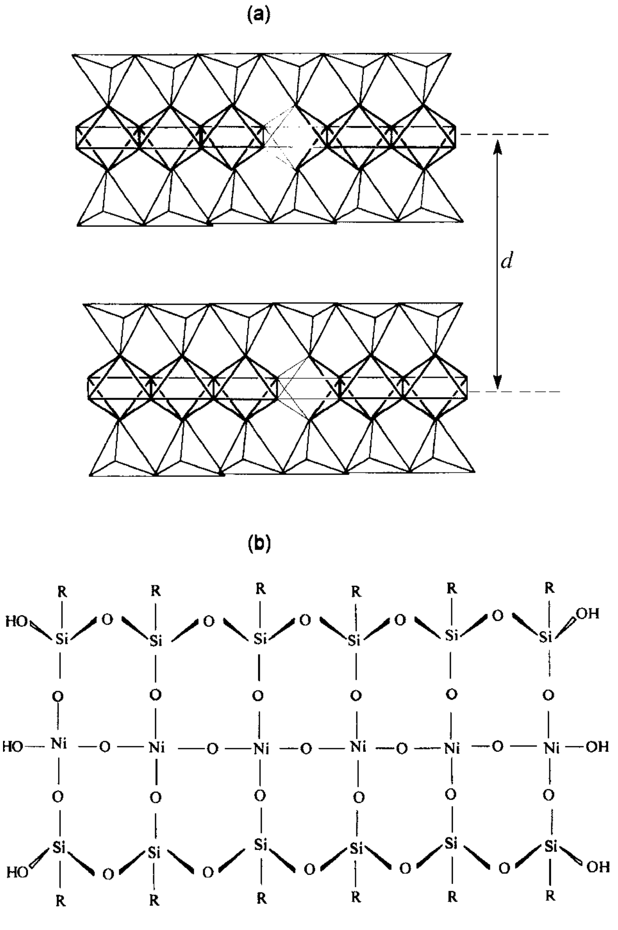

Fig. 5 Structure of nickel talc (a) and modified phyllosilicates (b), where R = $-CH_2CH_2CH_2NH_2$, $-CH_2CH_2CH_2NHCH_2CH_2NH_2$ or $-CH_2CH_2CH_2NHCH_2CH_2NHCH_2CH_2NH_2$ for SILNi*x* ($x = 1$–3).

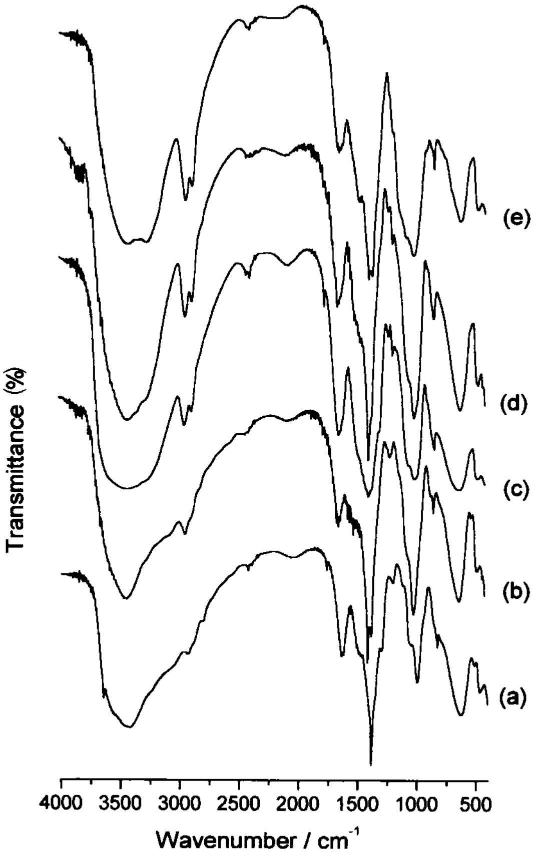

Fig. 6 IR spectra of modified phyllosilicates (a) SILNi1*, (b) SILNi1, (c) SILNi2*, (d) SILNi2 and (e) SILNi3. Hybrids (a) and (c) were synthesized at room temperature.

band. The asymmetric and symmetric [ν(C–H)] bands are assigned at 2938 and 2853 cm^{-1} and δ(Si–C)[28,29] is attributed to the band at 1200 cm^{-1}. The presence of intercalated nitrate groups was detected by a characteristic band at 1384 cm^{-1} while a band at 823 cm^{-1} is associated wth out of plane NO_2 bending.[30]

The vibrational spectra below 1000 cm^{-3} of some silicate containing minerals[31–33] contribute importantly to their characterization. Thus, for the synthesized phyllosilicates a sharp band in this region was attributed to the Si–O stretching vibration mode. On the other hand, a previous investigation involving the synthesis of nickel phyllosilicates showed that the Si–O stretching vibration band is shifted toward lower wavenumber, when the temperature of preparation was increased to 423 K.[34,35] However, the same band was not observed for our samples prepared at 323 K [Fig. 6(b), (d) and (e)]. For nickel silicates the presence of hydroxy groups bonded to nickel atoms of the inorganic structure leads to a well defined δ(NiO–H) band at 630 cm^{-1} and the Si–O stretching vibration mode[34,35] is responsible for the band at 470 cm^{-1}.

Both Si–O stretching and δ(NiO–H) vibrations depend on the nature of the phyllosilicate.[35] Two stretching bands appear for 1 : 1 nickel phyllosilicate at 1005 and 1035 cm^{-1}, while only one band was detected for the 2 : 1 structural arrangement at 1020 cm^{-1}. The region corresponding to δ(NiO–H) showed a band at 670 cm^{-1} for 1 : 1 nickel phyllosilicate whereas for the 2 : 1 formulation a doublet at 710 and 670 cm^{-1} was found. The present data show that ill-crystallized 1 : 1 and 2 : 1 nickel phyllosilicates cannot be distinguished by their δ(NiO–H) vibration modes which are located very close to 670 cm^{-1}. However, materials produced by condensation of the alkoxide precursors also present bands in the region 1000–1035 cm^{-1}.

The observed wavenumbers for δ(NiO–H) in SILNix matrices were lower, having a value of 670 cm^{-1}. The position of this band at lower frequencies can be attributed to hydrogen bonding between the structural hydroxy groups and the amino organic groups of the attached chains.

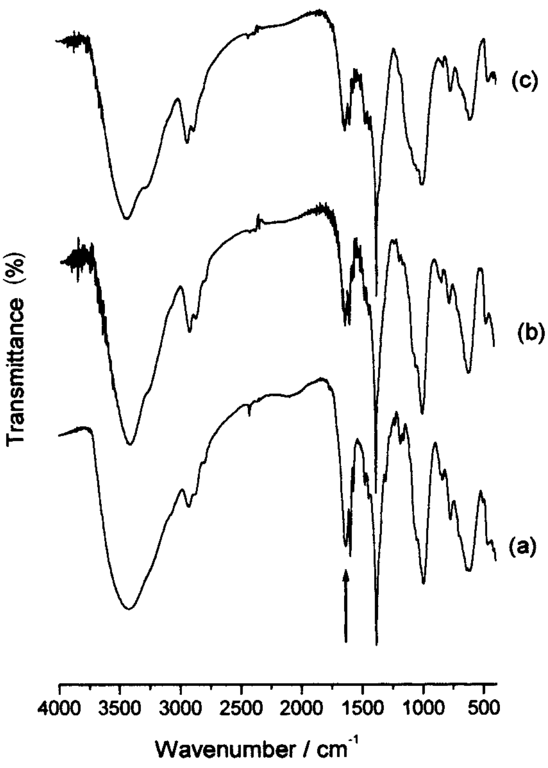

Fig. 7 IR spectra of phyllosilicates (a) SILNi1, (b) SilNi2 and (c) SILNi3 after reaction with 2-pyridinecarbaldehyde.

After reaction with 2-pyridinecarbaldehyde the resulting hybrids showed the presence of the –C=Npy functionality in the structure of the mineral as illustrated in Fig. 7. The appearance of new bands attributed to the aromatic C=C stretching frequencies were observed at 1590 and 1475 cm^{-1}. The sharp medium band at 1635 cm^{-1} is attributed to the C=N vibration mode while a new absorption at 773 cm^{-1} is provides evidence of the attached pyridinic ring on the pendant group.[36]

Thermal analysis

Thermal study of the organoclays showed that the minerals had DTG peaks with maxima at temperatures below 550 K. The thermogravimetric curves of these phyllosilicates gave mass losses of 43.0, 51.0 and 52.9 for SILNix (x = 1–3), respectively, between 298 and 1173 K. These results indicated that the degree of thermal degradation increases with the size of the chain of the organic group for the SILNix hybrids. The degradation stages are indicated in Table 3. The initial mass loss can be attributed to the release of water, and corresponds

Table 3 Weight loss, Δm and range of temperature, ΔT over which this occurs, for the hybrids obtained from thermogravimetry between 298 and 1220 K for samples synthesized at 323 K

Hybrid	ΔT/K	Δm (%)
SILNi1	298–443	9.00
	443–590	13.50
	590–773	20.36
SILNi2	298–418	8.60
	418–568	11.40
	568–1073	31.00
SILNi3	310–414	8.10
	468–713	29.52
	713–1219	15.24

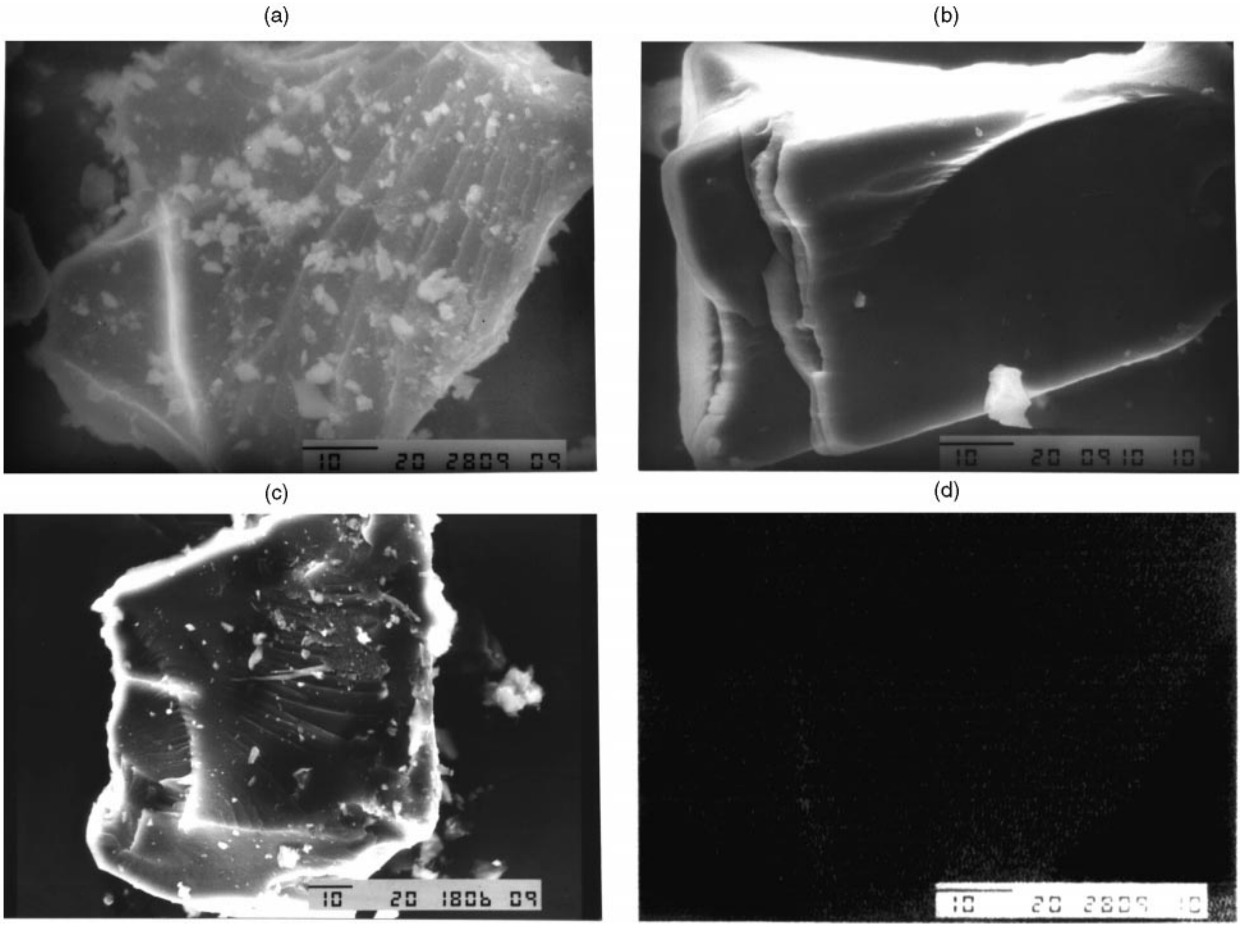

Fig. 8 Scanning electron micrographs of particles of (a) SILNi1, (b) SILNi2, (c) SILNi3 and (d) distribution map of nickel atoms in the SILNi1 matrix. The bar corresponds to 10 μm.

to *ca.* 9%. The subsequent release can be associated with further loss of water, as well as some of the organic groups. The second DTG peak was detected at 549, 543 and 539 K for SILNix ($x = 1$–3). The release of organic moieties occurred more readily with increase in chain length. A continuous decomposition of the SILNi3 material was obtained up to 713 K, to give a total loss of 29.52%. These processes on SILNi1 and SILNi2 hybrids occurred with lower mass loss in the same temperature range. However, the DTG peaks seem to indicate that the thermal decomposition processes were similar in nature. At temperatures >973 K, the nickel phyllosilicates may be transformed into a crystalline silicate (olivine) or amorphous silica and NiO.

NMR spectroscopy

The degree of hydrolysis of alkoxy groups of the precursor and the condensation between the silicate sheets can be, in principle, estimated using ^{29}Si NMR spectroscopy. However, the presence of the nickel ions in the phyllosilicate structure precluded analysis since nickel(II) is paramagnetic and causes substantial broadening of ^{29}Si signals.[31,32]

Scanning electron microscopy

SEM photomicrographs shown in Fig. 8(a)–(c) show well formed particles in all cases. The particles exhibit plate-like forms, possibly suggesting layered structures for these hybrids. Fig. 8(d) shows that nickel is uniformly dispersed in the SILNi1 matrix as indicated by the detected bright points. This behaviour was also observed for the other hybrids. The EDS spectrum shows the presence of two strong peaks identified as silicon and nickel in these hybrids.

Conclusion

Three analogous 2:1 layered nickel organosilicates were successfully prepared using a modified synthetic route at 323 K. According to XRD data, the hybrids have a layered structure, with changes in interlayer space which depend on the length of the organic chain attached to the trialkoxysilane group employed in the reaction. XRD data of SILNix ($x = 1$–3) also indicate a 2:1 trioctahedral arrangement.

Reaction of these hybrids with 2-pyridinecarbaldehyde was carried out and new bands in the IR spectra appeared at 1635 and 1590 cm^{-1}. XRD revealed an increase in the interlayer spacing peak due to the incorporation of new organic guest species into the gallery space.

Acknowledgements

The authors are indebted to FAPESP for financial support and CAPES-PICD (M.G.F.), FAPESP (C.R.S.) and CNPq (C.A.) for fellowships.

References

1 T. J. Pinnavaia, *Science*, 1983, **220**, 365.
2 A. Kadkhodayan, C.-L. Lin and T. J. Pinnavaia, in *Chemically Modified Surfaces in Science and Industry*, ed. D. E. Leyden and W. T. Collins, Gordon Breach Science, New York, 1988, vol. 2, p. 221.
3 P. Lazlo and J. Lucchetti, *Tetrahedron Lett.*, 1984, **25**, 2147.
4 M. Kawai, R. Ohno and Y. Izumi, *Tetrahedron Lett.*, 1988, **61**, 2157.
5 B. Velde, *Introduction to Clay Minerals*, Chapman & Hall, London, 1992.

6 Y. Fukushima and M. Tami, *J. Chem. Soc., Chem. Commun.*, 1995, 241.
7 Y. Fukushima and M. Tami, *Bull. Chem. Soc. Jpn.*, 1996, **69**, 3667.
8 S. L. Burkett, A. Press and S. Mann, *Chem. Mater.*, 1997, **9**, 1071.
9 L. Ukrainczyk, R. A. Bellman and A. B. Anderson, *J. Phys. Chem. B*, 1997, **101**, 531.
10 N. T. Whilton, S. L. Burkett and S. Mann, *J. Mater. Chem.*, 1998, **8**, 1927.
11 M. G. Fonseca, C. R. Silva and C. Airoldi, *Langmuir*, 1999, **15**, 5048.
12 G. W. Brindley, D. L. Bish and H.-M. Wan, *Am. Mineral.*, 1979, **64**, 615.
13 I. De Vynck, *Silic. Ind.*, 1980, **3**, 51.
14 A. Decarreau, *Bull. Miner.*, 1980, **103**, 579.
15 A. Decarreau, *Geochim. Cosmochim. Acta*, 1985, **49**, 1537.
16 T. Mizutani, Y. Fukushima, A. Okada and O. Kamigaito, *Bull. Chem. Soc. Jpn.*, 1990, **63**, 2094.
17 Y.-S. Hong and S.-J. Kim, *Bull. Korean Chem. Soc.*, 1997, **18**, 236.
18 T. P. Lishko, L. V. Glushchenko, Y. V. Kholin, Z. N. Zaitev, A. Bugaevskii and N. D. Donskaya, *Russ. J. Phys. Chem.*, 1991, **65**, 1584.
19 J. J. Yang, I. M. El-Nahhal, C. I-Ssuer and G. E. Maciel, *J. Non-Cryst. Solids*, 1997, **209**, 19.
20 M. G. Fonseca and C. Airoldi, *J. Chem. Soc., Dalton Trans.*, 1999, **21**, 3687.
21 JCPDS card number 15-384.
22 D. M. Moore and R. C. Reynolds, *X-Ray Diffraction and the Identification and Analysis of Clay Minerals*, Oxford Univ Press, London, 1997.
23 S. W. Bailey, in *The X-Ray Identification and Crystal Structures of Clay Minerals*, ed. G. Brown, Mineralogical Society, London, 1961, ch. 1.
24 JCPDS card number 14-117.
25 P. Génin, A. Delahaye-Vidal, F. Prometer, F. Tekaia and M. Figlarz, *Eur. J. Solid State Inorg. Chem.*, 1991, **28**, 505.
26 P. Burattin, M. Che and C. Louis, *J. Phys. Chem. B*, 1997, **101**, 7060.
27 JCPDS card number 22-444.
28 D. L. Pavia, G. M. Lampman and G. S. Kriz, *Introduction to Spectroscopy: A Guide for Students of Organic Chemistry*, Saunders College Publishing, Orlando, FL, 1996.
29 R. M. Silverstein, G. C. Bassler and T. C. Morrel, *Spectrometric Identification of Organic Compounds*, John Wiley & Sons, London, 1991.
30 K. Nakamoto, *Infrared Spectra of Inorganic and Coordination Compounds*, John Wiley & Sons, New York, 1986.
31 V. C. Farmer, *Spectrochim. Acta*, 1964, **20**, 1149.
32 P. J. Launer, *Am. Mineral.*, 1967, **51**, 765.
33 R. W. T. Wilkins and J. Ito, *Am. Mineral.*, 1967, **52**, 1649.
34 P. Gérard and A. J. Herbillon, *Clays Clay Miner.*, 1983, **31**, 143.
35 M. Kermarec, J. Y. Carriat, P. Burattin, M. Che and A. Decarreau, *J. Phys. Chem.*, 1994, **98**, 12008.
36 M. G. Fonseca and C. Airoldi, *J. Mater. Chem.*, 1999, **9**, 1375.

Paper a907804e